

The catalytic role of the distal site asparagine-histidine couple in catalase-peroxidases

Christa Jakopitsch¹, Markus Auer¹, Günther Regelsberger¹, Walter Jantschko¹, Paul G. Furtmüller¹, Florian Rüker² and Christian Obinger¹

¹Institute of Chemistry and ²Institute of Applied Microbiology, University of Agricultural Sciences, Vienna, Austria

Catalase-peroxidases (KatGs) are unique in exhibiting an overwhelming catalase activity and a peroxidase activity of broad specificity. Similar to other peroxidases the distal histidine in KatGs forms a hydrogen bond with an adjacent conserved asparagine. To investigate the catalytic role(s) of this potential hydrogen bond in the bifunctional activity of KatGs, Asn153 in *Synechocystis* KatG was replaced with either Ala (Asn153→Ala) or Asp (Asn153→Asp). Both variants exhibit an overall peroxidase activity similar with wild-type KatG. Cyanide binding is monophasic, however, the second-order binding rates are reduced to 5.4% (Asn153→Ala) and 9.5% (Asn153→Asp) of the value of native KatG [$4.8 \pm 0.4 \times 10^5 \text{ M}^{-1}\cdot\text{s}^{-1}$ at pH 7 and 15 °C]. The turnover number of catalase activity of Asn153→Ala is

6% and that of Asn153→Asp is 16.5% of wild-type activity. Stopped-flow analysis of the reaction of the ferric forms with H₂O₂ suggest that exchange of Asn did not shift significantly the ratio of rates of H₂O₂-mediated compound I formation and reduction. Both rates seem to be reduced most probably because (a) the lower basicity of His123 hampers its function as acid-base catalyst and (b) Asn153 is part of an extended KatG-typical H-bond network, the integrity of which seems to be essential to provide optimal conditions for binding and oxidation of the second H₂O₂ molecule necessary in the catalase reaction.

Keywords: catalase-peroxidase; *Synechocystis* PCC 6803; catalase activity; peroxidase activity; compound I.

On the basis of sequence similarities with yeast cytochrome *c* peroxidase (CCP) and plant ascorbate peroxidases (APXs), catalase-peroxidases (KatGs) have been shown to be members of class I of the superfamily of plant, fungal and bacterial heme peroxidases [1]. KatGs have been found in prokaryotes (archaeobacteria and eubacteria) and fungi and are homomultimeric proteins with monomers being twice as large as CCP or APXs adding up to about 79–85 kDa, which is ascribed to gene duplication [2]. From both CCP and APX the crystal structures have been solved [3,4] and, quite recently, the 2.0 Å crystal structure of the homodimeric KatG from *Haloarcula marismortui* has been published [5]. This structure and sequence alignments suggest that all class I peroxidases have conserved the amino-acid triad His, Asp and Trp in the proximal pocket and the triad Trp, Arg and His in the distal pocket (Fig. 1). Despite this homology, class I peroxidases dramatically differ in their reactivities towards hydrogen peroxide and

one-electron donors. Catalase-peroxidases have a predominant catalase activity but differ from monofunctional catalases in also exhibiting a substantial peroxidatic activity with broad specificity. However, no substantial catalase activity has ever been reported for either CCP or APX. Cytochrome *c* peroxidase (CCP) is unusual in that it prefers another protein (cytochrome *c*) as a redox partner, whereas ascorbate peroxidases (APXs) prefer the anion ascorbate as electron donor. But both cytochrome *c* and ascorbate are poor substrates for KatGs [6–8].

The initial step in the catalytic mechanism of a peroxidase and catalase is heterolysis of the oxygen-oxygen bond of hydrogen peroxide. This reaction causes the release of one water molecule and coordination of the second oxygen atom to the iron center [9]. The resulting intermediate, compound I, is two oxidizing equivalents above the resting state; two electrons have been transferred from the enzyme to the coordinated oxygen atom, one from the iron and one from either the porphyrin or an amino-acid residue [9]. With most peroxidases compound I is a ferryl (Fe^{IV}=O) porphyrin π -cation radical, whereas for some intermediates such as CCP compound I a ferryl (Fe^{IV}=O) protein radical has been reported [10]. Recently, residues in the putative distal active site of KatGs have been the targets of site-directed mutagenesis studies. The role of distal Trp, Arg and His was studied in the KatGs from *Escherichia coli* [11,12] and from the cyanobacterium *Synechocystis* PCC 6803 [12,13]. The data presented in these papers suggest that distal His and Arg in KatGs have a similar role in compound I formation as in other peroxidases [9].

The main difference in the catalase and peroxidase activity is compound I reduction. In the catalase cycle, a

Correspondence to C. Obinger, Institute of Chemistry, Metalloprotein Research Group, University of Agricultural Sciences, Muthgasse 18, A-1190 Vienna, Austria.

Fax: + 43 1 36006 6059, Tel.: + 43 1 36006 6073,

E-mail: christian.obinger@boku.ac.at

Abbreviations: KatG, catalase-peroxidase; APX, ascorbate peroxidase; CCP, cytochrome *c* peroxidase; HRP, horseradish peroxidase; CT1 (> 600 nm), long wavelength porphyrin-to-metal charge transfer band.

(Received 26 August 2002, revised 14 January 2003, accepted 22 January 2003)

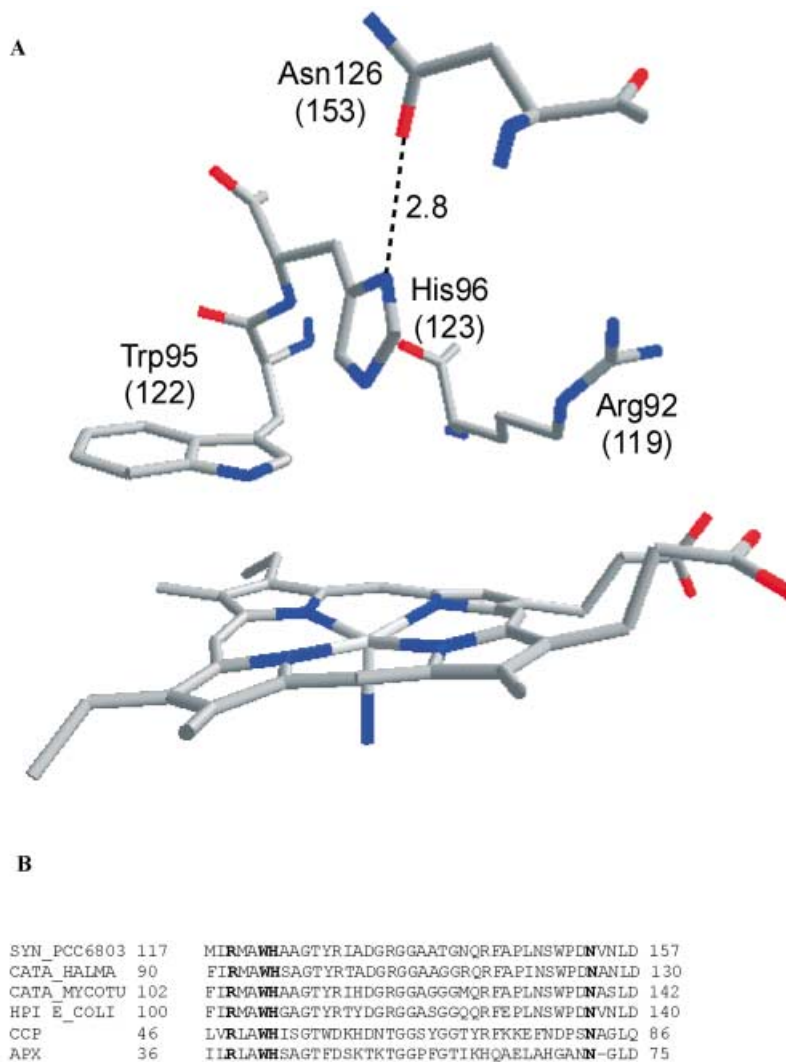


Fig. 1. Distal site structure of catalase-peroxidase from *Haloarcula marismortui*. The figure was constructed using the coordinates deposited in the Protein Data Bank (accession code 1ITK). The amino-acid numbering is for *Haloarcula* KatG, but numbers in parentheses denote numbering for *Synechocystis* KatG. Only one selected hydrogen bond is shown. (B) Multiple sequence alignment performed for all three branches of class I peroxidases. The overall amino-acid sequence identity between *Synechocystis* KatG and *Haloarcula* KatG is 55%. Selected residues conserved in all class I peroxidases are bold. Syn_PCC6803, KatG from *Synechocystis* PCC 6803; CATA_HALMA, KatG from *Haloarcula marismortui*; CATA_MYCOTU, KatG from *Mycobacterium tuberculosis*; HPI E_COLI, KatG from *Escherichia coli*; CCP, yeast cytochrome *c* peroxidase; APX, cytosolic pea ascorbate peroxidase.

second peroxide molecule is used as a reducing agent for compound I. This two-electron reduction completes the cycle forming the ferric enzyme and molecular oxygen, whereas in the peroxidase cycle, compound I is reduced in two consecutive one-electron steps via compound II back to the ferric enzyme. It has been demonstrated [11–13], that in KatGs the distal Trp is essential for the H₂O₂-mediated two-electron reduction step of compound I. The reasoning for this was based on the observations that in the Trp variants (a) the catalase activity was significantly reduced [11] or even lost [12,13], whereas (b) the ratio of peroxidase to-catalase activity was increased dramatically [11] indicating that compound I formation was not influenced by this mutation.

Alignment of amino-acid sequences and inspection of the crystal structures of members of the plant, fungal and bacterial superfamily show the existence of a hydrogen bond between the distal His and an Asn (Fig. 1) [3–5]. The corresponding residues in class I peroxidases are Asn82 (CCP), Asn72 (pea APX) and Asn153 in *Synechocystis* KatG (Fig. 1). Replacement of Asn82 of CCP [14,15] and Asn70 in horseradish peroxidase (HRP) [16,17] has been reported. Whereas with CCP the effect of disruption on the catalytic activity was not studied, the HRP mutants

Asn70→Val and Asn70→Asp showed decreased rates in compound I formation by hydrogen peroxide. Compounds I and II reduction by phenolic substrates were slower whereas reduction by ABTS [2,2'-azino-bis-(3-ethylbenzothiazoline-6-sulfonic acid)] was substantially increased.

As KatGs are the only peroxidases which are competent to reduce and oxidize hydrogen peroxide at a reasonable rate, it is important to understand the role of the H-bonding partners of the conserved distal site residues Trp, Arg and His. In this work Asn153 of KatG from *Synechocystis* PCC 6803 was replaced with Asp (Asn153→Asp) and Ala (Asn153→Ala). A comprehensive kinetic analysis of both the catalase and the peroxidase activity including multimixing stopped-flow spectroscopy is presented and discussed with respect to the extraordinary catalytic features of catalase-peroxidases.

Materials and methods

Reagents

Standard chemicals and biochemicals were obtained from Sigma Chemical Co. at the highest grade available.

Expression, purification of KatGs from *Synechocystis* and spectrophotometric characterization of wild-type and mutant proteins was described previously [13].

Mutagenesis

Oligonucleotide site-directed mutagenesis was performed using PCR-mediated introduction of silent mutations as described [13]. A pET-3a expression vector that contained the cloned catalase-peroxidase gene from the cyanobacterium *Synechocystis* PCC 6803 [7,13] was used as the template for PCR. At first unique restriction sites were selected flanking the region to be mutated. The flanking primers were 5'-AATGATCAGGTACCGGCCAGTAAATG-3' containing a *KpnI* restriction site and 5'-TGCATAAAGGATCCGGGTGC-3' containing a *BamHI* restriction site. The following mutant primers with the desired mutation and a silent mutation introducing a restriction site were constructed (point mutations italicized and restriction sites underlined): 5'-CTGAATTCCTGGCCAGATGCCGTCAATTTAGAC-3' and 5'-CCAGGAATTCAGGGGGCGAAGC-3' introduced the restriction site *EcoRI* and changed Asn153 to Ala; 5'-CCTGAATTCCTGGCCAGATGACGTCAATTTAGAC-3' and 5'-CCAGGAATTCAGGGGGGCGAAGC-3' introduced the restriction site *EcoRI* and changed Asn153 to Asp.

Steady-state kinetics

Catalase activity was determined polarographically in 50 mM phosphate buffer using a Clark-type electrode (YSI 5331 Oxygen Probe) inserted into a stirred water bath (YSI 5301B) at 25 °C. One unit of catalase is defined as the amount that decomposes 1 μmol of $\text{H}_2\text{O}_2 \cdot \text{min}^{-1}$ at pH 7 and 25 °C. Peroxidase activity was monitored spectrophotometrically using 1 mM H_2O_2 and 5 mM guaiacol ($\epsilon_{470} = 26.6 \text{ mM}^{-1} \cdot \text{cm}^{-1}$) or 1 mM *o*-dianisidine ($\epsilon_{460} = 11.3 \text{ mM}^{-1} \cdot \text{cm}^{-1}$). One unit of peroxidase is defined as the amount that decomposes 1 μmol of electron donor min^{-1} at pH 7 and 25 °C.

Transient-state kinetics

Transient-state measurements were made using the model SX-18 mV stopped-flow spectrophotometer from Applied Photophysics equipped with a 1-cm observation cell thermostated at 15 °C. This temperature was chosen to allow comparison with transient kinetic data of other KatG variants investigated under identical conditions. Calculation of pseudo-first-order rate constants (k_{obs}) from experimental traces at the Soret maximum was performed with the SpectraKinetic workstation v4.38 interfaced to the instrument. The substrate concentrations were at least five times that of the enzyme to allow determination of pseudo-first-order rate constants. Second-order rate constants were calculated from the slope of the linear plot of pseudo-first-order rate constants vs. substrate concentration. To follow spectral transitions a photodiode array accessory (model PD.1 from Applied Photophysics) connected to the stopped-flow machine together with the XSCAN DIODE ARRAY SCANNING v1.07 software was utilized. The kinetics of oxidation of ferric catalase-peroxidase to compound I by

peroxides (peroxoacetic acid or *m*-chloroperbenzoic acid) or the formation of the cyanide complex had to be followed in the single mixing mode. Catalase-peroxidase and the peroxide or cyanide were mixed to give a final concentration of 1 μM enzyme and 20–500 μM peroxide or 20–500 μM cyanide. The first data point was recorded 1.5 ms after mixing and 2000 data points were accumulated. Sequential-mixing stopped-flow analysis was used to measure compound I reduction by one-electron donors. In the first step the enzyme was mixed with peroxoacetic acid and, after a delay time where compound I was built, the intermediate was mixed with the electron donors aniline, ascorbate or *o*-dianisidine. All stopped-flow determinations were measured in 50 mM phosphate buffer, pH 7.0 and 15 °C, and at least three determinations were performed per substrate concentration.

Results

Spectral properties

Figure 2 depicts the UV-Vis spectra of wild-type KatG and the two variants investigated in this study. The absorption spectrum of the Asn153→Ala variant resembles closely that of the recombinant wild-type enzyme in the resting state [7,12,13] exhibiting the typical bands of a heme *b*-containing ferric peroxidase in the visible and near ultraviolet region. The Soret peak at 406 nm (small shoulder at 380 nm) together with two bands around 512 and 640 nm (CT1) suggest the presence of a dominating five-coordinate high-spin heme coexisting with some six-coordinate high-spin heme. The A_{406}/A_{280} ratio (i.e. Reinheitszahl) of Asn153→Ala varies between 0.46 and 0.48 from one preparation to another (wild-type protein: 0.57–0.61). The Reinheitszahl of Asn153→Asp is in the range 0.42–0.45 and the peaks in the UV/Vis spectrum are at 408, 512 and 640 nm. The small shoulder at 368 nm indicates the presence of some free heme corresponding with the slightly

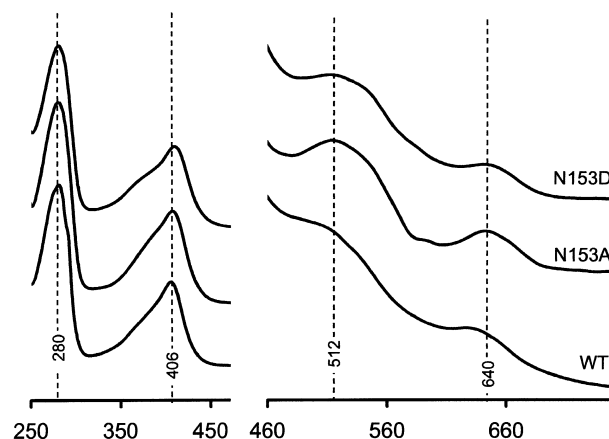


Fig. 2. UV-Vis spectra of the ferric forms of *Synechocystis* wild-type KatG and of the variants Asn153→Ala and Asn153→Asp. Conditions: Ferric proteins in 50 mM phosphate buffer, pH 7.0, and 25 °C. The absorbance ratio (A_{Soret}/A_{280}) of the proteins was 0.60 for wild-type KatG, 0.47 for Asn153→Ala, 0.44 for Asn153→Asp, respectively. The region between 460 and 700 nm has been expanded sixfold.

Table 1. Apparent K_m and k_{cat} values for the catalase activity of wild-type and variant catalase-peroxidases from *Synechocystis* PCC 6803. Also given are specific peroxidase activities (units per mg protein). Reaction conditions: 50 mM phosphate buffer, pH 7, and 30 °C. For catalase and peroxidase assays as well as unit definition see Materials and methods.

	Wild-type	Asn153→Ala	Asn153→Asp
Catalase activity			
K_m (mM H ₂ O ₂)	4.1 ± 0.2	1.7 ± 0.2	2.3 ± 0.3
k_{cat} (s ⁻¹)	3500 ± 350	200 ± 25	580 ± 34
k_{cat}/K_m (× 10 ⁵ M ⁻¹ ·s ⁻¹)	8.5	1.2	2.5
Peroxidase activity			
<i>o</i> -Dianisidine (μmol·min ⁻¹ ·mg ⁻¹)	3.8 ± 0.6	1.9 ± 0.6	4.3 ± 0.5
Guaiacol (μmol·min ⁻¹ ·mg ⁻¹)	0.6 ± 0.1	0.55 ± 0.09	0.6 ± 0.4

lower Reinheitszahl of Asn153→Asp. These spectral data together with the kinetic parameters presented below suggest that the mutations caused no significant changes in the interactions of the heme with the apoprotein. The protein yield was similar for all recombinant proteins (60–80 mg recombinant KatG from 1 L of *E. coli* culture).

Catalase and peroxidase activity

Recombinant KatG exhibits an overwhelming catalase activity. The polarographically measured specific catalase activity in the presence of 5 mM hydrogen peroxide is 1160 ± 55 U·mg⁻¹ of protein. With 100 μM H₂O₂ and 20 mM pyrogallol or 1 mM H₂O₂ and 5 mM guaiacol, the peroxidase activity was determined to be 6.6 ± 0.6 or 0.6 ± 0.1 U·mg⁻¹, respectively. Table 1 shows, what happens upon exchanging Asn153. Both variants exhibit a reduced catalase activity. Compared with wild-type KatG the k_{cat} values of Asn153→Ala and Asn153→Asp were determined to be 6% and 17%. Figure 3 shows the pH dependence of the catalase activity. The KatG-specific pH dependence with a maximum activity at pH 6.5 is seen with both Asn153→Asp and Asn153→Ala (not shown) indicating that the distal His in KatGs should not be one of the key residues responsible for this typical pH profile. The affect of mutation on the overall peroxidase activity can be neglected. Both mutants exhibited similar oxidation rates of guaiacol and *o*-dianisidine as the wild-type protein (Table 1).

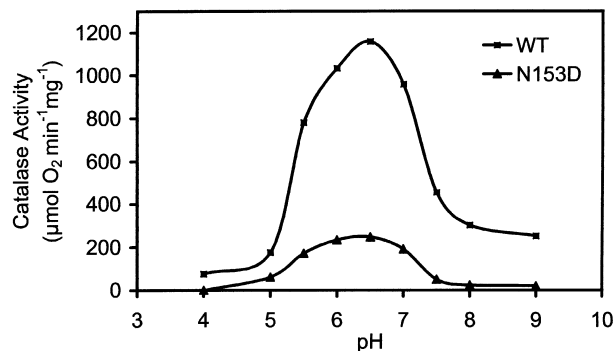


Fig. 3. pH profile for catalase activity of *Synechocystis* catalase-peroxidase. The specific catalase activity of wild-type KatG and the variant Asn153→Asp (N153D) is given in μmol O₂ formed per minute and mg protein as determined polarographically at 25 °C in 50 mM citrate-phosphate or Tris buffers, pH 4.0–9.0.

Cyanide binding

Cyanide is a useful probe to investigate the binding site of heme proteins. Figure 4A shows the spectral changes upon addition of cyanide to ferric wild-type KatG and Asn153→Ala. A similar low spin spectrum is obtained when Asn153→Asp is mixed with excess cyanide (not shown). The Soret peak of wild-type KatG shifts to 422 nm accompanied by a small hypochromicity (isosbestic point at 414 nm) and a prominent new peak at 542 nm is seen. The corresponding peaks of the cyanide complex of

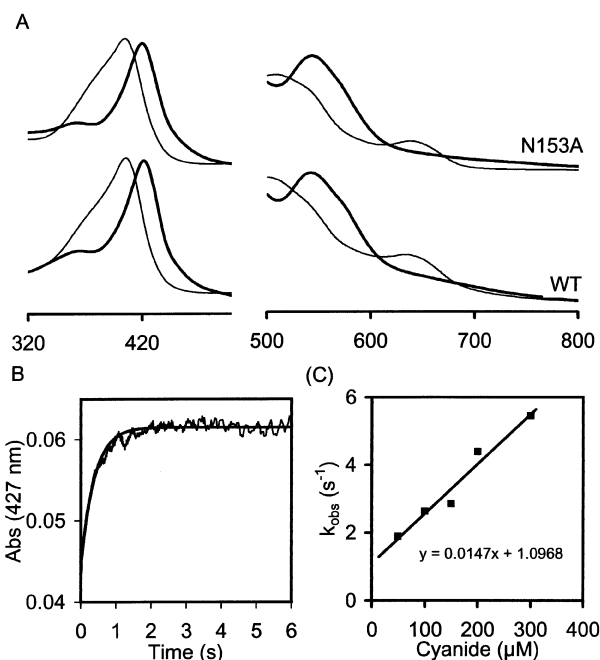


Fig. 4. Cyanide binding to the ferric forms of *Synechocystis* wild-type KatG and Asn153→Ala. (A) UV-Vis spectra of the ferric forms and cyanide complexes of *Synechocystis* wild-type KatG and Asn153→Ala. Conditions: ferric proteins (2 μM) were mixed with 10 mM cyanide in 100 mM phosphate buffer, pH 7.0, and 25 °C. The region between 460 and 700 nm has been expanded sixfold. (B) Typical time trace and fit of the reaction between Asn153→Ala (1 μM) and 100 μM cyanide followed at 427 nm in 50 mM phosphate buffer, pH 7.0, and 15 °C. (C) Pseudo-first-order rate constants for the formation of the cyanide complex of Asn153→Ala in 50 mM phosphate buffer, pH 7.0, and 15 °C.

Asn153→Ala are at 420 nm (isosbestic point at 413 nm) and 544 nm, respectively (Fig. 4A). Cyanide binding was monophasic and gave single exponential curves, indicating pseudo-first-order kinetics. A typical time trace followed at 427 nm (the maximum absorbance difference between the cyanide complex and the ferric protein) and the corresponding fit are shown in Fig. 4B. The observed rate of cyanide binding to the ferric enzyme linearly increased with the concentration of cyanide. The slope yielded the apparent second-order rate constant for cyanide binding (k_{on}). The value obtained for the wild-type enzyme is $(4.8 \pm 0.4) \times 10^5 \text{ M}^{-1}\cdot\text{s}^{-1}$ at pH 7 and 15 °C. The finite intercept (7.6 s^{-1}) represents k_{off} . From the ratio $k_{\text{off}}/k_{\text{on}}$ a value for the dissociation constant of the cyanide complex to ferric enzyme and cyanide of $15.8 \mu\text{M}$ was calculated. The present data unequivocally demonstrate that Asn153 plays a role in cyanide binding. In both variants cyanide binding was monophasic (see single exponential fit in Fig. 4B; normalized variance = 3.95×10^{-7}), but the binding rate was drastically reduced (Fig. 4C). With Asn153→Ala a binding rate of $(1.5 \pm 0.4) \times 10^4 \text{ M}^{-1}\cdot\text{s}^{-1}$ and a dissociation constant of $74.6 \mu\text{M}$ was calculated. With Asn153→Asp similar values were determined [$k_{\text{on}} = (4.6 \pm 0.5) \times 10^4 \text{ M}^{-1}\cdot\text{s}^{-1}$ and $k_{\text{off}}/k_{\text{on}} = 80.4 \mu\text{M}$].

Compound I formation

As has been reported recently, the catalase activity of wild-type KatGs does not allow to follow compound I formation by addition of hydrogen peroxide [7,12,13]. However, upon addition of peroxyacetic acid a compound I spectrum can be obtained that is distinguished from the resting state by a 40–50% hypochromicity and its formation can be followed as exponential absorbance decrease at the Soret maximum. This is shown for wild-type *Synechocystis* KatG in Fig. 5B. In case of Asn153→Ala and Asn153→Asp with an excess of peroxyacetic acid these stopped-flow experiments also give single exponential curves (Fig. 5C) and the plots of the pseudo-first-order rate constants, k_{obs} , vs. peroxyacetic acid concentration are linear with very small intercepts (Fig. 5D). From the slope the bimolecular rate constants were calculated to be $(2.6 \pm 0.3) \times 10^4 \text{ M}^{-1}\cdot\text{s}^{-1}$ (Asn153→Ala) and $(4.2 \pm 0.4) \times 10^4 \text{ M}^{-1}\cdot\text{s}^{-1}$ (Asn153→Asp) at pH 7 and 15 °C. As Table 2 demonstrates these rates are similar to wild-type KatG. By contrast, compound I formation mediated by m-chloroperbenzoic acid is faster in both Asn153→Ala and Asn153→Asp compared with wild-type KatG (Table 2). However, neither with peroxyacetic acid (Fig. 5A) nor with m-chloroperbenzoic acid a hypochromicity of 40–50% could be obtained as is the case with the wild-type protein. The maximum observed hypochromicity was 19%. Nevertheless, the formed redox intermediate was stable for seconds and allowed to study its reactivity with electron donors using the sequential-mixing stopped-flow technique.

Compound I reduction

In a typical experiment, 4 μM recombinant protein was premixed in the aging loop with 400 μM peroxyacetic acid and, after a delay time of 3 s, the electron donor was added. Similar to earlier observations with wild-type KatG and

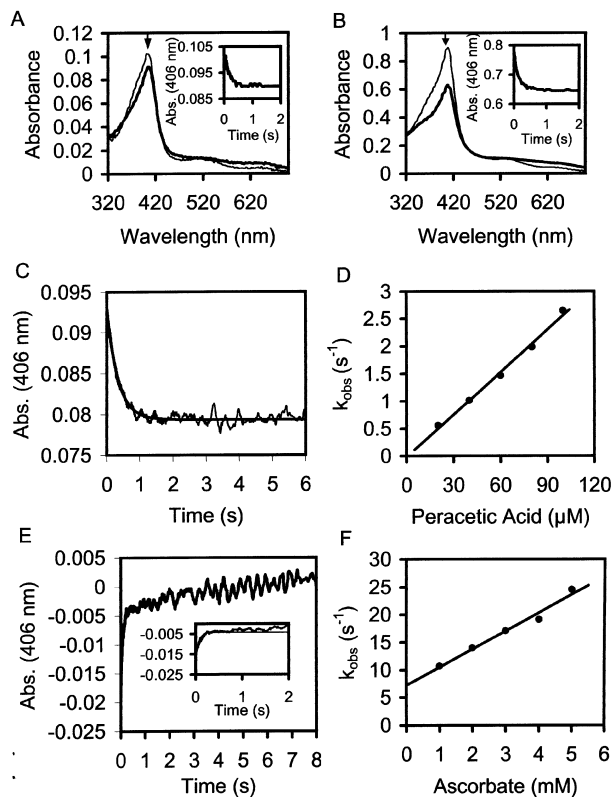


Fig. 5. Compound I formation and reduction of wild-type *Synechocystis* KatG and Asn153→Ala. (A) Spectral changes upon addition of peroxyacetic acid to ferric Asn153→Ala. Final concentrations: 100 μM peroxyacetic acid and 1 μM Asn153→Ala. First spectrum is that of ferric enzyme. Second spectrum (bold) is that of compound I and was taken after 1 s. The inset shows the corresponding time trace at 406 nm and 15 °C (50 mM phosphate buffer, pH 7.0). (B) Spectral changes upon addition of peroxyacetic acid to ferric wild-type KatG. Final concentrations: 100 μM peroxyacetic acid and 10 μM wild-type protein. First spectrum is that of ferric enzyme. Second spectrum (bold) is that of compound I and was taken after 2 s. The inset shows the corresponding time trace at 406 nm and 15 °C (50 mM phosphate buffer, pH 7.0). (C) Original time trace (406 nm) and single exponential fit of the reaction between 1 μM ferric Asn153→Ala and 100 μM peroxyacetic acid at 15 °C and pH 7.0. (D) Pseudo-first-order rate constants for the formation of Asn153→Ala compound I plotted against peroxyacetic acid concentration. (E) Original time trace (406 nm) of the reaction between 1 μM ferric Asn153→Ala compound I and 2 mM ascorbate at 15 °C (50 mM phosphate buffer, pH 7.0). The inset shows the exponential phase and fit used to calculate the k_{obs} values. (F) Pseudo-first-order rate constants for the Asn153→Ala compound I reduction plotted against ascorbic acid concentration.

distal mutants [7,12,13], addition of classical one-electron donors to compound I resulted in the formation of a redox intermediate with spectral features that did not resemble a typical (red-shifted) compound II spectrum known from other peroxidases (e.g. horseradish peroxidase or APX) but was similar to the ferric protein. The Soret band remains at 406 nm, however, the extinction coefficient is between that of compound I and the ferric protein. Consequently, compound I reduction of both Asn153→Ala and Asn153→Asp has been followed at 406 nm. A typical time

Table 2. Bimolecular rate constants of compound I formation and reduction of wild-type *Synechocystis* KatG and the variants Asn153→Ala and Asn153→Asp (50 mM phosphate buffer, pH 7, and 15 °C). Compound I was formed with peroxyacetic acid and its reactivity was tested by using the sequential-mixing stopped-flow method (for details see Materials and methods).

	Wild-type	Asn153→Ala	Asn153→Asp
Compound I formation ($\times 10^3 \text{ M}^{-1}\cdot\text{s}^{-1}$)			
Peroxyacetic acid	39 \pm 4	26 \pm 3	42 \pm 4
<i>m</i> -Chloroperbenzoic acid	53 \pm 8	157 \pm 14	180 \pm 19
Compound I reduction ($\times 10^3 \text{ M}^{-1}\cdot\text{s}^{-1}$)			
Aniline	14 \pm 6	68 \pm 6	18 \pm 5
<i>o</i> -Dianisidine	2710 \pm 350	3400 \pm 840	3670 \pm 950
Ascorbate	5.4 \pm 1.9	4.0 \pm 0.9	5.1 \pm 0.6

trace with ascorbate as electron donor is shown in Fig. 5E. Inspection of the time trace shows that the reaction is biphasic exhibiting an exponential increase (which could be attributed to compound II formation) followed by a slow conversion back to the ferric enzyme. The slow phase fits well with the observation that ascorbate is generally a very poor substrate of KatGs. In order to obtain actual bimolecular rate constants which could represent the one-electron reduction of compound I to compound II the first exponential phase was fitted (see inset to Fig. 5E) and the pseudo-first-order rate constants plotted against the electron donor concentration (Fig. 5F). The finite ordinate intercept in Fig. 5F could represent the rate of compound I reduction in the absence of exogenous substrates. As Table 2 shows unequivocally, mutation of Asn153 in *Synechocystis* KatG had only minor effects on compound I reduction. Both the order of magnitude as well as the hierarchy of donors (ascorbate < aniline << *o*-dianisidine) is very similar in wild-type KatG and both variants.

Discussion

The most prominent difference between peroxidases and other heme proteins is the high reactivity towards hydrogen peroxide. One of the essential features of this reactivity is acid-base catalysis by a conserved distal histidine which is located in the distal cavity and facilitates the deprotonation of H₂O₂ forming an initial Fe-OOH complex and finally assists in the heterolytic cleavage of the O–O bond by protonating the distal oxygen [18]. A similar role plays the distal His in KatGs as has been demonstrated recently by site-directed mutagenesis [11,13]. It plays a significant role in the distal H-bonding of KatGs which also involves water molecules and the conserved distal Trp and Arg [19]. In addition, as suggested by the published structure of KatG from *Haloarcula marismortui* and sequence alignments (Fig. 1), the distal His123 of *Synechocystis* KatG is hydrogen-bonded via its N₈H to Asn153, an amino acid a bit far from the immediate vicinity of the heme (Fig. 1).

Indeed, the kinetic parameters determined in this work confirm the proposal that Asn153 is part of the distal H-bond network in KatGs and is an important structural determinant in the multifunctional activity of KatGs [13,19]. Firstly, disruption of the hydrogen bond between Asn153 and His123 reduces the overall catalase activity by about one order of magnitude, whereas the influence on the overall

peroxidase activity is apparently neglectable. Secondly, in the variants Asn153→Ala and Asn153→Asp the binding constants for cyanide to the ferric protein is about an order of magnitude lower than the corresponding binding constant of wild-type KatG. As the basicity of the distal histidine is important in both hydrogen peroxide reduction (i.e. compound I formation) and cyanide binding, it is reasonable to assume that the disruption of the H-bond makes the distal His less basic. As a consequence the pK_a value of the N₈H of the distal His is lowered and the rate constant for the reaction with hydrogen peroxide and cyanide is reduced. The line of reasoning that the H₂O₂-mediated compound I formation is slower in the Asn153 variants can only be indirect because of the intrinsic high catalase activity. Only when amino-acid exchanges diminish the rate of compound I reduction by H₂O₂ (i.e. exchange of distal Trp [12] or proximal Trp [23]), the oxidation of ferric KatG by hydrogen peroxide can be followed. In this respect both Asn153→Ala and Asn153→Asp behave such as wild-type KatG and do not allow to follow this reaction. However, similar data obtained with both CCP and HRP underline the proposed role of Asn153 in KatG catalysis. NMR spectroscopy clearly showed that in the CCP variant Asn82→Asp the hydrogen bond between the N_ε of His52 and heme-coordinated cyanide has been eliminated [14]. As a consequence of mutation this CCP variant was shown to exist in at least three forms and their dynamic interconversion being controlled by pH, temperature and isotopic effects [20]. Binding constants of fluoride and cyanide were decreased in this CCP variant [15]. Unfortunately, no kinetic data about H₂O₂-mediated compound I formation of this variant are available and also no kinetic parameters regarding the peroxidase activity in CCP Asn82→Asp or a corresponding APX variant. Nevertheless, investigations of the class III model enzyme HRP and the Asn70→Val and Asn70→Asp variants [16,17] unequivocally demonstrated that the rates of compound I formation were reduced to about 10% of the value of native HRP. All these findings suggest a similar role of the distal Asn-His couple in plant-type peroxidases.

The present work also clearly showed that the basicity of the distal His has no impact on the reduction of organic peroxides. With peroxyacetic acid the same rates were obtained in wild-type and both mutant proteins, and with *m*-chloroperbenzoic acid even higher rates were obtained in the Asn153 variants. Generally, only little differences between Asn153→Ala and Asn153→Asp were observed

with regard to their spectroscopic properties and reactivities, though principally Asp is a potent hydrogen bond acceptor. The crystal structure of CCP [3] indicates that Asn82 donates another hydrogen bond to the peptide carbonyl oxygen atom of Glu76. This hydrogen bond also exists in pea APX (Glu65) [4] and, based on the *Haloarcula* KatG structure and sequence alignments, exists in *Synechocystis* KatG (Leu147) and helps to additionally anchor the distal His in the optimum position. It is reasonable to assume that in Asn153→Asp the Asp residue is deprotonated at the polar distal site and therefore cannot act as a hydrogen donor to the peptide group of Leu147. As a consequence Asp cannot compensate the role of Asn and the distal His is destabilized to the same extent in both Asn153→Ala and Asn153→Asp. A more open cavity could result and explain the higher reactivity towards the more bulky organic peroxides such as *m*-chloroperbenzoic acid.

At the moment we cannot explain why the organic peroxides induce a hypochromicity of the Soret Band of at most 20% compared to 40–50% in compound I formation of wild-type KatG. We exclude that only a fraction of the protein in its ferric form has been oxidized or that the mutations induced a marked compound I instability (meaning that we have observed a steady-state spectrum and not that of pure Asn153→Ala or Asn153→Asp compound I). This reasoning is based on (a) inspection of the spectra of the ferric forms, (b) the stopped-flow observations that demonstrated that Asn153→Ala or Asn153→Asp compound I were stable for seconds, (c) that the formed intermediate exhibited the same reactivity towards one-electron donors as the wild-type intermediate, and finally (d) that with cyanide a nearly 100% monophasic transition to the low spin complex could be observed. More likely are differences in the heme environment in wild-type and mutant compound I caused by the poor anchoring of distal His in both Asn153→Ala and Asn153→Asp. As a consequence the spectroscopic features of compound I could be changed.

So the question remains how the disruption of the hydrogen bond between His123 and Asn153 affects compound I reactivity. No effect of mutation was observed when one-electron donors were added to compound I. This is in contrast to the HRP mutants Asn70→Val [21] and Asn70Asp [16] where compound I reduction rates by phenolic substrates were reduced to less than 10% compared to wild-type HRP. This is thought to be based on the decreased basicity of the distal His that depresses the proton abstraction from the donor (which precedes electron transfer from the substrate to the heme in HRP [22]). Thus, from the data of this work one may conclude that the distal His in KatGs is not essential in the deprotonation step during compound I reduction by phenolic donors.

However, replacement of Asn153 seems to reduce the rate of hydrogen peroxide oxidation by compound I (i.e. the catalase reactivity). This is deduced from the fact that the overall catalase but not peroxidase activity is reduced upon manipulation of Asn153. As changes in the rate of compound I formation should have the same impact on both catalase and peroxidase activity, it is reasonable to assume that in both Asn153→Ala and Asn153→Asp also the H₂O₂-mediated reduction of compound I is diminished. This fits well with recent observations that in most variants

the consequence of amino-acid exchange in the heme cavity is a reduced catalase activity [12,13,19,23]. Recent spectroscopic investigations on *Synechocystis* KatG variants (exchanges of Arg119, Trp122 and His123 [19]) showed the existence of a pronounced H-bonding pattern at the distal heme side involving also His123. The present work unequivocally suggest that Asn153 is part of this network. It is reasonable to assume that disruption of the hydrogen bond between Asn153 and His123 has a strong influence on this H-bonding network. Its disturbance impairs the conditions for binding and oxidation of the second H₂O₂ molecule necessary in the catalase reaction of this unique peroxidase.

This proposed role of Asn153 is completely different from that of its neighbour Asp152. Figure 1B shows that in KatGs the distal Asn is part of the triad Pro-Asp-Asn (in *Synechocystis* KatG Pro151-Asp152-Asn153). Asn is found in all plant-type peroxidases, whereas Asp is conserved only in KatGs. In CCP a serine substitutes the aspartate forming the triad Pro80-Ser81-Asn82 and in APX an alanine substitutes the aspartate giving the triad Gly69-Ala70-Asn71, respectively (Fig. 1B). Preliminary investigations about the role of this conserved distal aspartate showed, that in Asp152 variants H₂O₂ oxidation was much slower than H₂O₂ reduction (manuscript in preparation), which is in contrast to wild-type KatG and the Asn153 variants described in this paper. Asp152 seems to participate directly in the H₂O₂ oxidation reaction (i.e. the catalase activity) whereas Asn153 participates indirectly in both the H₂O₂ reduction (by enabling the distal histidine to function as acid-base catalyst) and H₂O₂ oxidation (by stabilizing the KatG-typical H-bond network which is essential in the catalase activity).

Acknowledgements

This work was supported by the Austrian Science Funds (FWF project P15417).

References

1. Welinder, K.G. (1992) Superfamily of plant, fungal and bacterial peroxidases. *Curr. Opin. Struct. Biol.* **2**, 388–393.
2. Welinder, K.G. (1992) Bacterial catalase-peroxidases are gene duplicated members of the plant peroxidase superfamily. *Biochim. Biophys. Acta* **1080**, 215–220.
3. Finzel, B.C., Poulos, T.L. & Kraut, J. (1984) Crystal structure of yeast cytochrome *c* peroxidase refined at 1.7-Å resolution. *J. Biol. Chem.* **259**, 13027–13036.
4. Patterson, W.R. & Poulos, T.L. (1995) Crystal structure of recombinant pea cytosolic ascorbate peroxidase. *Biochemistry* **34**, 4331–4341.
5. Yamada, Y., Fujiwara, T., Sato, T., Igarashi, N. & Tanaka, N. (2002) The 2.0 Å crystal structure of catalase-peroxidase from *Haloarcula marismortui*. *Nat. Struct. Biol.* **9**, 691–695.
6. Obinger, C., Regelsberger, G., Strasser, G., Burner, U. & Peschek, G.A. (1997) Purification and characterization of a homodimeric catalase-peroxidase from the cyanobacterium *Anacystis nidulans*. *Biochem. Biophys. Res. Commun.* **235**, 545–552.
7. Jakopitsch, C., Rükner, F., Regelsberger, G., Dockal, M., Peschek, G.A. & Obinger, C. (1999) Catalase-peroxidase from the cyanobacterium *Synechocystis* PCC 6803: cloning, overexpression

- in *Escherichia coli*, and kinetic characterization. *Biol. Chem.* **380**, 1087–1096.
8. Engleder, M., Regelsberger, G., Jakopitsch, C., Furtmüller, P.G., Rümer, F., Peschek, G.A. & Obinger, C. (2000) Nucleotide sequence analysis, overexpression in *Escherichia coli* and kinetic characterization of *Anacystis nidulans* catalase-peroxidase. *Biochimie* **82**, 211–219.
 9. Dunford, H.B. (1999) *Heme Peroxidases*. Wiley-VCH, New York.
 10. Sivaraja, M., Goodin, D.B., Smith, M. & Hoffman, B.M. (1989) Identification by ENDOR of Trp191 as the free-radical site in cytochrome *c* peroxidase compound ES. *Science* **245**, 738–740.
 11. Hillar, A., Peters, B., Pauls, R., Loboda, A., Zhang, H., Mauk, A.G. & Loewen, P.C. (2000) Modulation of the activities of catalase-peroxidase HPI of *Escherichia coli* by site-directed mutagenesis. *Biochemistry* **39**, 5868–5875.
 12. Regelsberger, G., Jakopitsch, C., Furtmüller, P.G., Rümer, F., Switala, J., Loewen, P.C. & Obinger, C. (2001) The role of distal tryptophan in the bifunctional activity of catalase-peroxidases. *Biochem. Soc. Trans.* **29**, 99–105.
 13. Regelsberger, G., Jakopitsch, C., Rümer, F., Krois, D., Peschek, G.A. & Obinger, C. (2000) Effect of distal cavity mutations on the formation of compound I in catalase-peroxidases. *J. Biol. Chem.* **275**, 22854–22861.
 14. Satterlee, J.D., Alam, S.L., Mauro, J.M., Erman, J.E. & Poulos, T.L. (1994) The effect of the Asn82→Asp mutation in yeast cytochrome *c* peroxidase studied by proton NMR spectroscopy. *Eur. J. Biochem.* **224**, 81–87.
 15. Delauder, S.F., Mauro, J.M., Poulos, T.L., Williams, J.C. & Schwarz, F.P. (1994) Thermodynamics of hydrogen cyanide and hydrogen fluoride binding to cytochrome *c* peroxidase and its Asn-82→Asp mutant. *Biochem. J.* **302**, 437–442.
 16. Nagano, S., Tanaka, M., Ishimori, K., Watanabe, Y. & Morishima, I. (1996) Catalytic roles of the distal site asparagine–histidine couple in peroxidases. *Biochemistry* **35**, 14251–14258.
 17. Tanaka, M., Nagano, S., Ishimori, K. & Morishima, I. (1997) Hydrogen bond network in the distal site of peroxidases: spectroscopic properties of Asn70→Asphorseradish peroxidase mutant. *Biochemistry* **36**, 9791–9798.
 18. Poulos, T.L. & Kraut, J. (1980) The stereochemistry of peroxidase catalysis. *J. Biol. Chem.* **255**, 8199–8205.
 19. Heering, H.A., Indiani, C., Regelsberger, G., Jakopitsch, C., Obinger, C. & Smulevich, G. (2002) New insights into the heme cavity structure of catalase-peroxidase: a spectroscopic approach to the recombinant *Synechocystis* enzyme and selected distal cavity mutants. *Biochemistry* **41**, 9237–9247.
 20. Satterlee, J.D., Teske, J.G., Erman, J.E., Mauro, J.M. & Poulos, T.L. (2000) Temperature, pH, and solvent isotope effects on cytochrome *c* peroxidase mutant N82A studied by proton NMR. *J. Protein Chem.* **19**, 535–542.
 21. Nagano, S., Tanaka, M., Watanabe, Y. & Morishima, I. (1995) Putative hydrogen bond network in the heme distal site of horseradish peroxidase. *Biochem. Biophys. Res. Commun.* **207**, 417–423.
 22. Dunford, H.B. (1982) Horseradish peroxidase: structure and kinetic properties. In *Peroxidases in Chemistry and Biology*, Vol. II (Everse, J., Everse, K.E. & Grisham, M.B., eds), pp. 1–24. CRC Press, Boca Raton, Florida.
 23. Jakopitsch, C., Regelsberger, G., Furtmüller, P.G., Rümer, F., Peschek, G.A. & Obinger, C. (2002) Engineering the proximal heme cavity of catalase-peroxidase. *J. Inorg. Biochem.* **91**, 78–86.